SERBIAN JOURNAL OF ELECTRICAL ENGINEERING
Vol. 20, No. 1, February 2023, 107-126

UDC: 621.316.722.1/.4 DOI: https://doi.org/10.2298/SJEE2301107A

Embedded Control System for Reactive Power Control in Distributed Energy Resources for Voltage Regulation in the Distributed Power System

Vasanth Arumugam[1], Ashok Kumar[1]

Abstract: Since more distributed energy resources (DER) are being linked to the electrical grid, the current distributed power system (DPS) is encountering additional voltage regulation challenges. Traditionally, on-load tap changers, step voltage regulators, and switched capacitor banks have been used for voltage regulation in DPS. However, these sources are insufficient for voltage regulation in current DPS. As a result, reactive power assistance from a DER unit based on power electronics is intended to adjust the voltage in the DPS. In terms of flexibility, security, reliability, and availability, embedded control systems are now being investigated by researchers for use in power converter-fed DER units. This paper presents a method for constructing an embedded controller unit based on XynergyXS for the power converter controller, which includes reactive power regulation in the DER unit. Furthermore, it proposes dynamic reactive power control in the DER unit for enhanced DPS voltage regulation. The suggested voltage control approach is tested in a MATLAB/Simulink model of a practical 85-bus distributed power system located in the northern Tamilnadu region, India as well as a modified IEEE 33-bus system. The new control approach investigates all potential power grid disruptions. The results reveal that the proposed reactive power control method in DER units enhances network voltage regulation while reducing the number of switching operations performed by static voltage regulating units such as on load tap changers and switched capacitor banks.

Keywords: Grid voltage regulation, Static voltage regulating devices, Distributed energy resources, Embedded control, Reactive power control system.

1 Introduction

The ability to supply electric power to consumers is a fundamental role of distributed power systems, and it is currently facing additional issues because of the inclusion of distributed energy resources (DERs) such as variable wind, solar photovoltaic (PV) resources, and so on. The quantity of wind and solar PV

[1]Electrical Engineering Department, Annamalai University, Tamilnadu, India- 608002;
E-mails: realvasanth@gmail.com; ashokraj_7098@rediffmail.com

generation connected to the grid has expanded dramatically in the twenty-first century due to the clean energy vision, the dream of electricity for all, and enhanced control technology. Through innovation, these DER units assist in offering electricity to all people throughout the world while also increasing the energy efficiency of the power system [1]. Nonetheless, because of the nature of renewable power generation variability, these DERs represent a risk to the distributed power system. Voltage instability caused by DER's intermittent power generation is one of the key challenges to the distributed power system [2]. It is noted that voltage instability can cause power system blackouts, as witnessed, and demonstrated by many instances. On load tap changers (OLTC) and switched capacitor (SCB) or inductor banks (SIB) have traditionally been used to regulate the voltage of a power system, and these voltage regulating sources are known as static voltage regulating sources. However, modern distributed power systems rely heavily on DER units and power generation is time-variable in nature. Therefore, dynamic voltage regulating resources are necessary in addition to traditional ways for successful voltage control [3]. Furthermore, typical static voltage regulating resources face additional hurdles in the DER-rich network due to mechanical and electrical concerns. As a result, through IEEE 1547-2018, the IEEE DER work group and policymakers have given a regulation for reactive power support from power electronic-based DER units, which may offer dynamic voltage support to the grid during unforeseen scenarios [4].

Several studies on regulating reactive power in DER units have been conducted, including: (i) volt-var control mode, (ii) constant reactive power support mode, (iii) constant power factor mode, (iv) active power-reactive power mode, and so on [4, 5]. Furthermore, more research has been undertaken into the parallel functioning of DER reactive power support and static voltage support devices (OLTC, SCB) for effective voltage control [6 – 10]. Ref. [6] provided a strategy for managing voltage control in the German distributed power system by combining and coordinating the operation of solar PV units with reactive power assistance and an OLTC unit. It has evaluated the switching operations of OLTC units with various events in a day with the existence of a solar PV network, and it demonstrates that OLTC operations are effectively decreased by adjusting the reactive power support of a solar PV unit. The coordinated functioning of OLTC units and solar PV reactive power support through remote control is investigated in [7], and it is discovered that voltage regulation is performed successfully with fewer OLTC operations. Online voltage management for the combined functioning of DER reactive power support, SCB, and OLTC units for the Australian power system for improved voltage regulation was investigated in [8] and proved that combined operation of these voltage regulating devices led to improved voltage stability and reduced the number of switching operations of static voltage regulating devices. Aziz et al. suggested a combined centralized and local voltage control of a distributed power system using reactive power assistance from DER units, achieving voltage regulation during unexpected occurrences and power fluctuations, among other things, [9]. The unintended operations of OLTC due to the reactive power support from solar PV plants are described in [10]. It shows that the improper control of reactive power support from the DER units led to an increase in the number of switching operations of the static voltage regulating units. The energy saving estimation through the proper control of static voltage regulating devices and DER units is discussed in [11], and it shows that reactive power support from DER units significantly reduces the energy losses as well as reduces the active power demand in the DPD. [12] discusses robust volt/var control without centralized computations. It demonstrates that the specified technique has significantly reduced the voltage violations in the DPS compared with the traditional IEEE-based volt/var control strategy. A two-stage volt/var control strategy is performed in [13] by coordinating smart inverter-fed PVs and static voltage regulating devices. The specified voltage control strategy was tested in an IEEE 123-bus system, and the results revealed that the suggested method has improved the voltage stability at the point of common connection.

On the other hand, embedded controllers have gained renewed attention in the modern power converter control system because of their control flexibility and reliability. It is to be mentioned that the embedded controller additionally provides condition monitoring, defect detection, and data analysis functions in addition to its core goal, system control. Microcontroller units (MCUs) and field programmable gate arrays (FPGAs) are extensively used as embedded controls in power converter control systems [14]. The recent developments in the digital control for the DC/DC converter are reviewed in [15]. In addition, it has presented advantages for the digital controller, including online efficiency optimization, controller auto tuning, etc. Youn et al. suggested a digital predictive current control for the power factor correction techniques, [16]. It has been demonstrated that the suggested digital control system significantly reduces the total harmonic distortion. The direct digital controller for the bidirectional grid-connected modular multilevel converter is presented in [17] and it efficiently regulates the DC bus voltages through the current tracking principle. Ryal et al. proposed a digital closed-loop control strategy for the boost converter in power factor correction applications [18]. It showed that the digital control is implemented in a low-cost microcontroller, and further performance of the converter operation is improved with the proposed digital control method. The higher resolution digital pulse width modulation for the wind band gap semiconductor devices is presented in [19] and reveals the various advantages for the different applications. The enhancement of power converter cybersecurity through the parallel operation of digital model predictive control and analogue proportional integral controller is suggested in [20], and it has achieved better dynamic performance during normal operation and provides reliable control during cyber-attack events.

1.1 Problem description and contribution

As examined in the literature, a suitable reactive power control strategy is required from the DER unit for the modern distributed power system considering voltage stability, energy losses, and unintended operations of static voltage regulating devices. Most research works on DER reactive power control strategy are considered static in the literature, and DER units provide a limited amount of reactive power support to the power grid based on IEEE 1547-2018 recommendations [4], considering transient stability, unintended operations to static voltage regulating devices, and so on. As per IEEE regulations, the maximum reactive power support from a DER unit is limited to 0.44 p.u. of its unit capacity provided with the mandatory active power generation. This might lead to challenging and energy-efficient issues in the modern power system. For example, during peak load hours (19.00 PM to 21.00 PM), there is no active power generation from the solar PV unit, and therefore, reactive power support from the solar PV unit to the power grid is to be zero as mandated by IEEE recommendation. Traditionally, during such peak load periods, reactive power support and voltage regulation are achieved through static voltage regulating devices such as OLTC and SCB units. It might lead to an increase in the number of switching operations of these units. Furthermore, when voltage issues occur in the power grid (due to sudden load variations or distributed faults in the DPS), these units practically operate after the 20s to 30s. During this 20s period, grid voltage may go out of the stipulated voltage region (i.e., between 0.95 p.u. and 1.05 p.u.) and result in heating the electrical equipment connected to the DPS. In the worst case ((high R/X ratio or weak power grid), it might destabilize the distributed power system if suitable reactive power support is not provided within the certain period.

However, if the solar PV unit has a suitable reactive power control strategy with the vast utilization of reactive power support, then it might reduce the number of switching operations of static voltage regulating devices as well as maintain the voltage stability through the provision of reactive power support without affecting other voltage regulating equipment. As a result, this paper proposed the dynamic and extensive use of reactive power control strategies in the DER unit while preserving active power generation. Furthermore, the control system behind the reactive power support is based on the digital controller, which further improves the performance of the proposed control strategy in view of flexibility, health management of the DER unit, and cyber security, etc.

The goal of this paper is to establish the voltage regulation of the DPS through an embedded controller based dynamic reactive power controller in the DER unit as well as coordination with the static voltage regulating devices through time delay control. The paper's contributions are as follows: (i) developing an embedded control system for power converter fed DER units that includes closed loop control of the reactive power section; (ii) time-graded control of static voltage regulators; (iii) dynamic grid voltage support to the distributed power system during unexpected events via the proposed reactive power control strategy; and (iv) maximizing the utilization of reactive power support from DER units without affecting real power generation.

1.2 Structure of the paper

The work is arranged as follows: Part II discusses the theoretical view of voltage support from DER units. Section III outlines the characteristics of the embedded control system fed converter unit that will be used in the DER units. Section IV analyses the proposed voltage control strategy in the DER unit, while Section V offers the performance assessment findings of the proposed voltage control strategy in the DER unit via time domain simulation studies in the practical 85-bus northern Tamilnadu distributed power system, and Section VI summarizes the conclusion statement.

2 Change in Grid Voltage Caused by DER Reactive Power Feed-In

This section discusses the theory of voltage variance in the grid caused by DER unit reactive power provision. Fig. 1 shows an example. The simplified distributed power system diagram includes a fixed voltage source V_S, a DER unit, and two impedances Z_X and Z_Y, where the impedance connected between the voltage source and the DER is referred to as the upstream grid impedance Z_X, and the impedance from the DER to the load and load impedance is referred to as the downstream grid impedances Z_Y. The DER unit is seen as a current source, with I_P and I_Q managing the unit's active and reactive power. The mesh current analysis approach is employed to determine the voltage fluctuation at node V_{CC}.

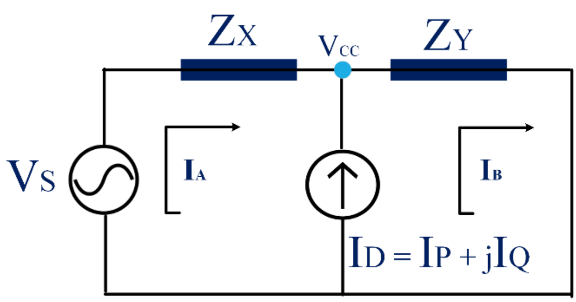

Fig. 1 – *Simplified power grid schematic.*

Mesh current analysis is performed in Fig. 1 and loop currents are calculated as

$$I_A = \frac{V_S - I_D Z_Y}{Z_X + Z_Y}, \tag{1}$$

$$I_B = \frac{V_S + I_D Z_X}{Z_X + Z_Y}. \tag{2}$$

The voltage at node V_{CC} is given as

$$V_{CC} = V_S - I_A Z_X, \tag{3}$$

$$V_{CC} = V_S - \frac{V_S Z_X}{Z_X + Z_Y} + \frac{I_D Z_X Z_Y}{Z_X + Z_Y}. \tag{4}$$

The first two terms in (4) are dependent on the fixed voltage source (V_S), while the third term is dependent on the DER unit. As a result, the voltage changes at V_{CC} caused by the DER unit are expressed as

$$V_{CC\_D} \cong \left[I_P + \mathrm{j} I_Q \right] \left[\frac{Z_X Z_Y}{Z_X + Z_Y} \right]. \tag{5}$$

The impedance can be recognized by its own resistance R and reactance X.

$$Z_X = R_X + \mathrm{j} X_X, \qquad Z_Y = R_Y + \mathrm{j} X_Y$$

Substitute Z_X and Z_Y, (5) can be rewritten and simplified as

$$\frac{V_{\mathrm{CC\_D}}}{I_P} = \frac{R_X \left[R_Y^2 + X_Y^2 \right] + R_Y \left[R_X^2 + X_X^2 \right]}{\left[R_X + R_Y \right]^2 + \left[X_X + X_Y \right]^2}, \tag{6}$$

$$\frac{V_{\mathrm{CC\_D}}}{I_Q} = \frac{X_X \left[R_Y^2 + X_Y^2 \right] + X_Y \left[R_X^2 + X_X^2 \right]}{\left[R_X + R_Y \right]^2 + \left[X_X + X_Y \right]^2}. \tag{7}$$

The voltage fluctuation at the point of common connection owing to the DER active (P) and reactive power (Q) feed-in is shown in (6) and (7), respectively.

Fig. 2 depicts the voltage change caused by the 100 kVA active and reactive power feed-in. DER units with an R/X ratio of the power grid are specified at 1. The grid's base voltage is 11 kV. Using the figures, sending inductive reactive power to the grid instead of capacitive reactive power or vice versa can result in a 5.498% difference in V_S at the point of common connection. In addition, expanding the reactive power could reduce the active (real) power generation of such DER units. Currently, DER units can support 0.44 p.u. unit capacity of the reactive power framed by IEEE 1547-2018, which follows (8):

$$Q_{grid} = -\frac{(0.44\ \text{p.u.}) \cdot (\text{active power generation})}{0.2\ \text{p.u.}}. \tag{8}$$

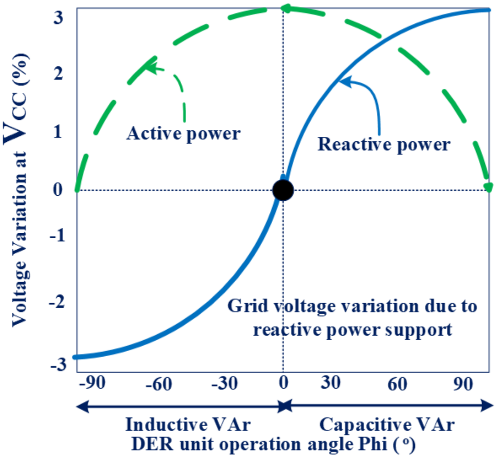

Fig. 2 – *Voltage variation at point of common connection due to active and reactive power feed-in power grid.*

As per IEEE 1547-2018, DER units can provide static reactive power support to the grid up to 0.44 p.u. of the unit capacity. However, it is noted that static reactive power support cannot be given to the power grid immediately after the voltage issues occur in the DPS. It can be given to the grid after 3s, as recommended by the IEEE workgroup.

3 Embedded Controller for Power Converter Used in DER Units

Because of the growing computing capacity in programmable control units such as digital signal processing, field programmable gate array (FPGA), and microcontrollers, among others, researchers are refocusing on the control of power converters utilizing embedded controllers. When compared to analogue control systems, embedded controller units give greater flexibility. Additionally, these controllers provide more extra features, such as system health monitoring, self-diagnosis, data analysis, and so on. Required computing performance is the primary determinant of controller selection for centralized embedded control systems.

A microcontroller unit (MCU) is designed specifically for power converter control applications, and it includes a controller with high-resolution pulse width modulators (i.e., switching frequencies of up to megahertz), adaptable analog/digital and digital/analog converters, communication peripherals, and an analogue trip section. Because the MCU's computational load power is triggered by supplementary features such as data monitoring and communication multiples, an MCU with multiple processing cores is a viable solution for a power converter fed DER centralized controller unit. Nonetheless, the MCU has a problem with the high control loop execution rate. On the other hand, a programmable logic system (for example, an FPGA) may be used as a control unit since it provides a versatile and adaptable system controller platform. The FPGA-created system controls are executed in parallel, allowing many independent control system implementations at the same time, reducing reaction time, and significantly improving control system execution rate. Despite the FPGA's extraordinary flexibility, the control unit produced may be noticeably slower as compared to the microcontroller-oriented solution due to the extensive growth of all peripherals. Furthermore, the programmable logic technique necessitates the use of extra parts for system control, such as analog-to-digital converters and bus driver units, which raises the cost of the method.

As a result, an MCU coupled to an FPGA may be used for the control system used in power converters feeding DER units, providing flexibility in control system design. The MCU performs tasks such as digital filtering, signal processing, instance signal conversions, and control loop processing. It has been noticed that FPGA is typically employed in applications that require a high control loop execution rate. In this study, MCU and FPGA are merged to give a better control system for the converter unit, which in this case is XynergyXS. The controller unit has an ARM Cortex-M4 based STM32F4 microcontroller with a clock frequency of 168 MHz and a Xilinx Spartan 6 series FPGA with a clock frequency of 250 MHz. The MCU handles control functions such as system condition monitoring, power stage management, AD conversions of measurement signals, and signal processing, whereas the FPGA handles PWM module for active front-end converters and voltage source inverters. The control system circuit schematic for the grid-connected voltage source converters utilized in DER units is shown in Fig. 3. The real (active) and reactive power of the power converters linked together in the DER units are controlled by this control system.

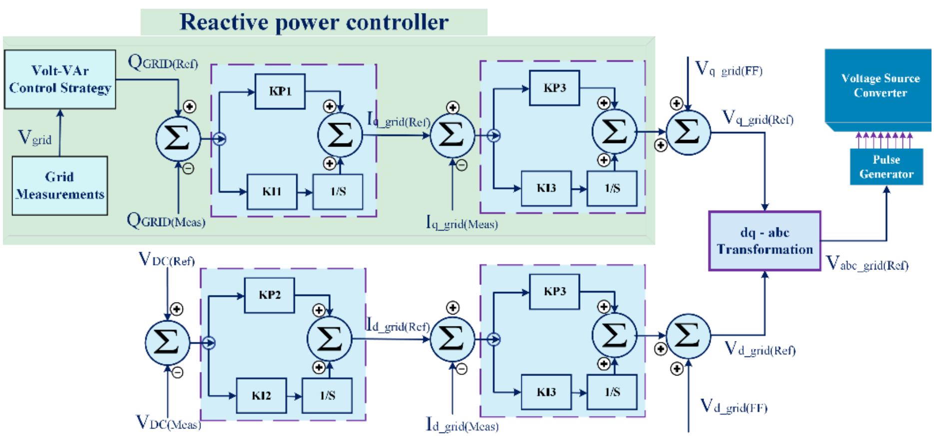

Fig. 3 – *Control circuit diagram for the grid connected voltage source converter.*

The DC link voltage control system is used to govern the power converter unit's dc link voltage as well as reactive power control, which regulates the grid voltage via reactive power support. In Fig. 3, the reactive power current controller has a greater bandwidth than the outer loop controller to preserve system stability. The reactive power reference is calculated using the grid voltage and provided via various reactive power control schemes. Volt-var control is used in this study, and a new control technique based on reactive power control is proposed. The Glover-McFarlane loop shaping approach is used to build the volt-var reactive power controller in the converter unit, which is a two-stage process. Stage-1: An open loop system with a weighing function is created to achieve the desired frequency domain characteristics; stage-2: As the plant distress increases, the weighing function becomes more difficult. Because this method typically yields a very high-order controller, model reduction techniques can be applied.

3.1 Digital PWM

Fig. 4a depicts a simplified build of a digital PWM modulator, and it consists of a clock signal, a binary comparator, and a binary counter. The duty cycle is calculated based on the operation of the converter, and it is processed in the software. When the timer count reaches the duty cycle, a gate signal with a variable period is created as shown in Fig. 4b. The conventional digital PWM technique has shortcomings in delay. Therefore, multi-sampling is employed to minimise delay.

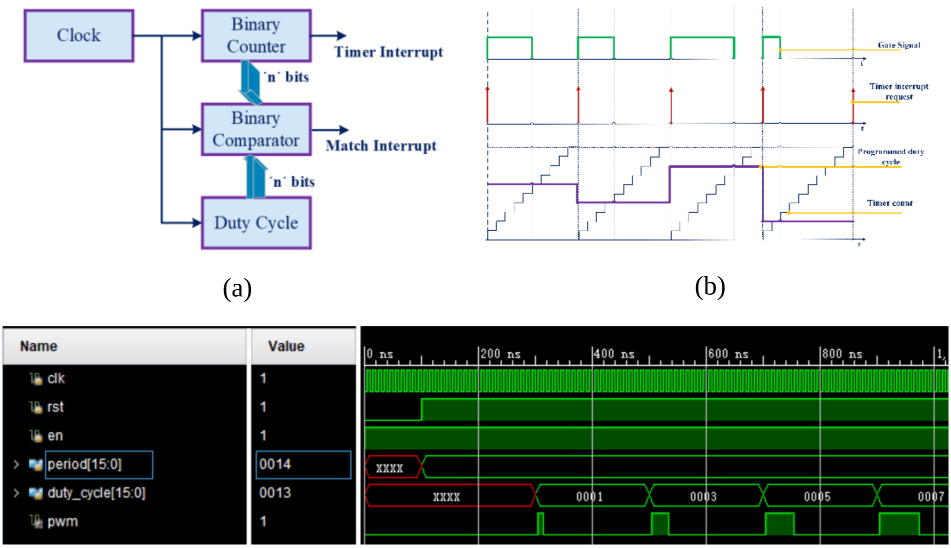

(a) (b)

(c)

Fig. 4 – *The digital PWM: (a) Blocks representation; (b) signal representation; (c) Simulation results of DPWM in Verilog language.*

The continuous modulating signal is held by ZOH (zero order holder), which is sampled into discrete flat modulating signal pieces. This signal is then compared to the carrier wave to create the modified signal. Because the goal is to output the DPWM control signal through an FPGA, the control module must be coded in HDL and the design must be synthesized. For this project, the Verilog programming language was selected. The DPWM generator module is built on the DPWM concept stated above. A testbench is created to test the DPWM generator module. The graphic depicts the simulation in Fig. 4c. We can observe that the length of the high PWM signal rises with each clock cycle as the duty cycle increases.

3.2 Digital current controller implementations

A digital PI controller can be designed from the analog controller in conjunction with adding suitable discretization methods such as forward Euler, backward Euler, and Tustin, etc. [21, 22]. The use of this approach results in some accuracy loss, owing mostly to the discretization process and the approximation in the corresponding continuous time delay representation. As the initial part of digital controller design, proportional and integral parameter values are estimated through analog control, and then they will be used in the digital controllers. The block diagram of the digital current controller loop with the PI controller is shown in Fig. 5.

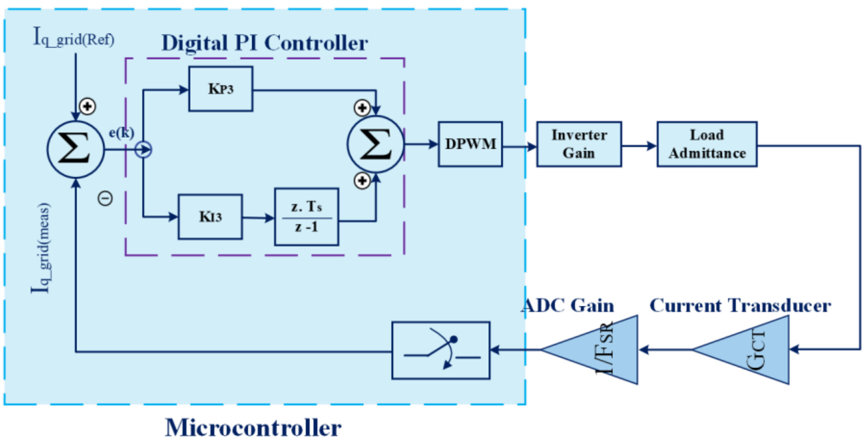

Fig. 5 – *Block diagram of digital current controller with PI regulator.*

Based on PI parameter calculation, proportional parameter (K_P) and integral parameter (K_I) values are selected as 2.01 and 2160 rads/s, respectively. The transfer function is given by:

$$PI(s) = K_I \frac{1 + K_p / K_I}{s} \quad . \tag{9}$$

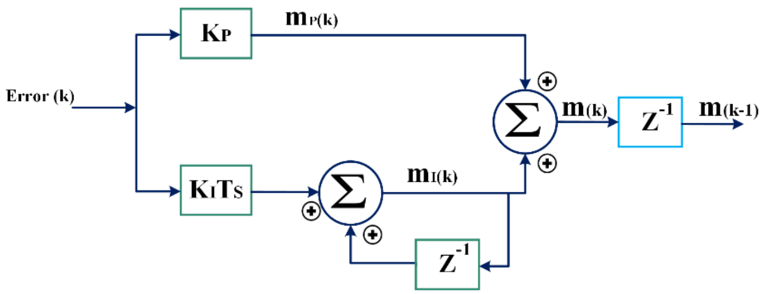

Fig. 6 – *Block diagram representation of the digital PI controller.*

In this paper, we might conduct controller discretization using the backward Euler integration approach. Therefore, the transfer function in (9) is modified into:

$$PI(z) = K_p + K_I T_S \frac{z}{z-1}. \tag{10}$$

T_S is the sampling time, and parameter ´*z*´ refers to *Z*-transform features.

For a better understanding, discrete-time regulator realization is considered, followed by a model of the computation delay. The control algorithm can be deferred based on *Z*-transform features represented in Fig. 6.

$$\begin{gathered} m_I(k) = K_I T_S e_I(k) + m_I(k-1), \\ m(k) = m_I(k) + m_P(k) = K_P e_I(k) + m_I(k). \end{gathered} \tag{11}$$

Finally, given a suitable analogue PI regulator, any of the studied discretization necessitates the computation of the digital PI gains as follows:

$$\begin{gathered} K_{I\_digital} = K_I T_S, \\ K_{P\_digital} = K_P. \end{gathered} \tag{12}$$

In this manner, the digital controller’s loss compared to the analogue controller may be reduced, resulting in a considerable performance boost.

4 Proposed Volt-Var Control Strategy in DER unit

The proposed voltage control approach in a DER-rich distributed power system is presented in this section. Based on the grid requirements, the proposed reactive power control in the DER unit may provide both static and dynamic reactive power assistance to the distributed power system. In addition, a time-graded control mechanism is provided between the DER reactive power control unit and static voltage regulating devices such as OLTC and SCB units. The effective time delay is considered for each unit to lessen the negative operations of OLTC and SCB units.

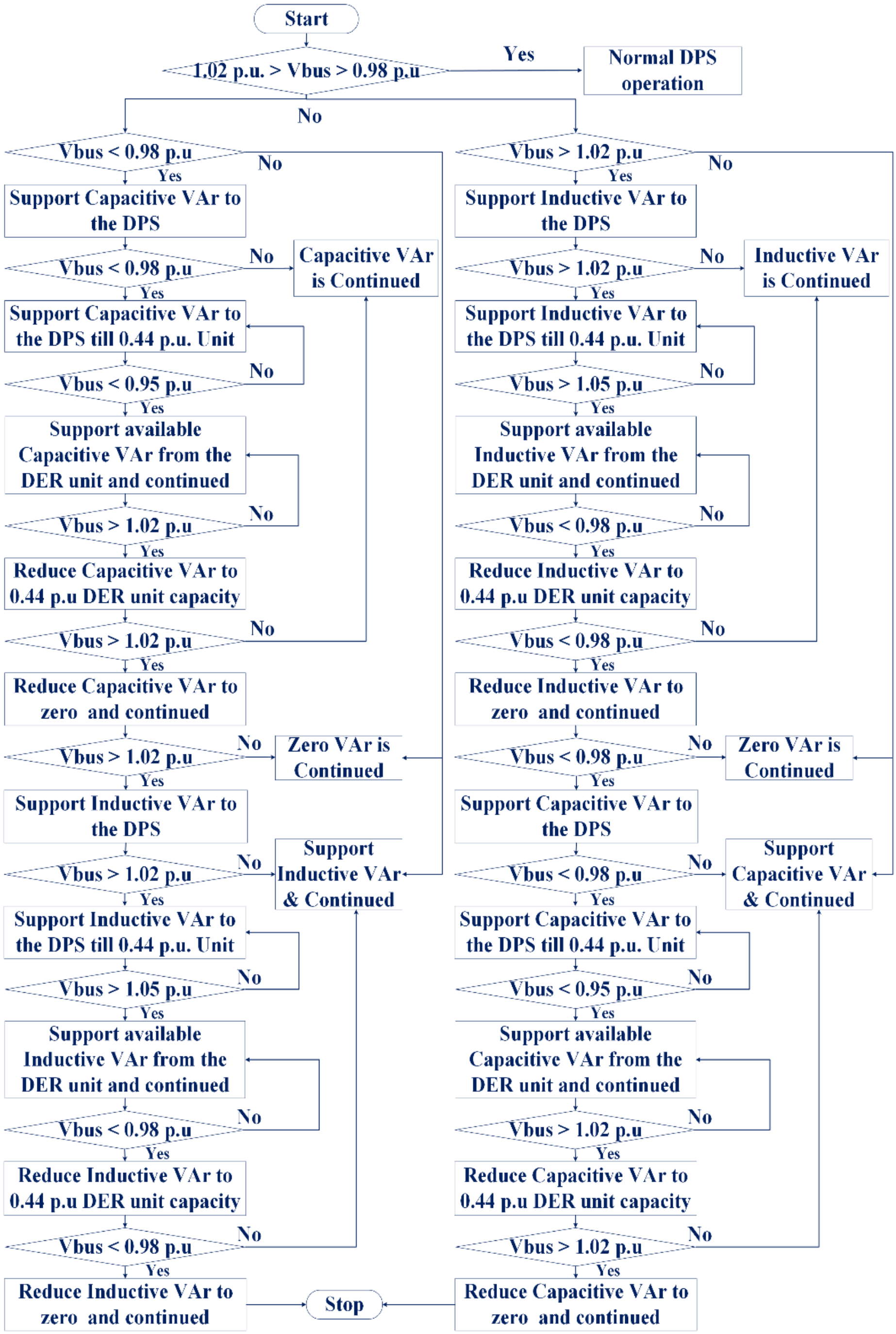

Fig. 7 – *Proposed volt-var control strategy in DER units.*

Fig. 7 depicts the proposed voltage control technique, which may offer both dynamic and static reactive power supply to the distributed power system. It uses the volt-var control method. When the voltage is less than 0.95 p.u., DER reactive power control is triggered, giving capacitive reactive power to the power system instantly. However, if the voltage is greater than 1.05 p.u., it delivers inductive reactive power to the grid. If the grid requires constant voltage support, the instantaneous voltage support is maintained. Otherwise, the DER unit will reduce the reactive power support to the grid (either capacitive or inductive) depending on the grid voltage. The voltage control approach used here is known as hysteresis type control, and it lowers grid oscillatory activities during instantaneous reactive power supply. The switching of the switched capacitor/inductor bank and the on-load tap changer are both delayed by 20s and 30s, respectively. As a result, if the grid requires extra voltage support, static voltage regulating devices such as SCBs and OLTCs are engaged.

Furthermore, the proposed control strategy provides instantaneous reactive power support to the grid based on the active power variation as given in (13). A DER unit's active power variation may be calculated by comparing present active power generation to regular day generation. The *R*/*X* value is constant, is determined by line characteristics (Thevenin equivalent impedance of the bus from the main power plant) and is not affected by load. Although the line's resistance is temperature dependent and fluctuates with loading, it is deemed minimal. If active power variation can be calculated dynamically, then dynamic reactive power assistance is possible in DER units during active power variation. Furthermore, using an appropriate control system, this dynamic reactive power supply may be used to minimize capacitor switching transients.

$$\Delta Q_{DER} \approx -\Delta P_{DER}\left(\frac{R}{X}\right). \tag{13}$$

Moreover, the proposed control technique is adequately justified under unbalanced voltage circumstances because reactive power support from DER units is calculated based on positive and negative sequence voltage, which leads to a reduction in grid voltage imbalance. The positive (V_{PCC}^{+}) and negative (V_{PCC}^{-}) sequence voltages of the point of common connection are determined using a three phase PLL system.

$$\Delta Q_{DER} \approx K^{+}\left(V_{PCC}^{+}\right) + K^{-}\left(V_{PCC}^{-}\right), \tag{14}$$

$$K^{-} = 1 - K^{+},\ K^{+} \text{ varies from 0 to 1,}$$

where K^{+} and K^{-} are the normalised factors needed to balance the positive and negative sequence voltages. The right selection of these parameters contributes to improved voltage balancing among phase voltages. The K^{+} value selection is based on the practical constraints as shown below.

$$\begin{Bmatrix} K^{+}=1 & \alpha \le 0.02 \\ 1>K^{+}>0 & 0.02<\alpha<1 \\ K^{+}=0 & \alpha=1 \end{Bmatrix}, \quad \alpha=\frac{V_{PCC}^{-}}{V_{PCC}^{+}}. \tag{15}$$

The Q-V curve is used to determine the relationship between change in reactive power and change in voltage in the DPS, which can be beneficial in limiting the maximum reactive power support from DER units in terms of system stability.

The power flow equations are considered for analyzing the Q-V relationship in a simple two-node three-phase distributed power system

$$\begin{aligned} P_{12} &= |V_1|^2 G - |V_1||V_2| G\cos(\theta_1-\theta_2) + |V_1||V_2| B\sin(\theta_1-\theta_2), \\ Q_{12} &= |V_1|^2 B - |V_1||V_2| B\cos(\theta_1-\theta_2) - |V_1||V_2| G\sin(\theta_1-\theta_2), \end{aligned} \tag{16}$$

where G and B are represented as the conductance and susceptance of the power system, respectively. If the system is considered ideal, $G = 0$. Therefore, (16) is modified as

$$\begin{aligned} P_{12} &= |V_1||V_2| B\sin(\theta_1-\theta_2), \\ Q_{12} &= |V_1|^2 B - |V_1||V_2| B\cos(\theta_1-\theta_2), \end{aligned} \tag{17}$$

$$\begin{aligned} P_{DER} &= -P_{21} = -|V_1||V_2| B\sin(\theta_2-\theta_1), \\ Q_{DER} &= -Q_{21} = -|V_2|^2 B + |V_1||V_2| B\cos(\theta_1-\theta_2). \end{aligned} \tag{18}$$

The required Q-V curve relationship of the DER units is drawn based on the value of V_1 and P_{DER} through (18).

5 Simulation Results and Discussions

To examine the proposed voltage control strategy in the distributed power systems, a modified IEEE 33-bus system as well as a practical 85-bus distributed power system located in the northern Tamilnadu region, India is considered as test systems, and they are simulated in MATLAB/Simulink via time domain simulation studies. The OLTC and SCB units are employed in both the test systems, where the deliberate time delay for such units' operation is considered as 30s and 20s, respectively. In addition, the selection time for each tap change in the OLTC unit is set to 5s, and the time between each SCB activation is assumed to be 2s.

5.1 Test System 1: A modified IEEE 33-bus system

A 10 MVA synchronous generator is considered as the primary electrical power source of this distributed power system, as well as two solar PV units rated at 1.25 MVA and 1.2 MVA, which are connected on bus 14 and bus 32, respectively, as shown in Fig. 8.

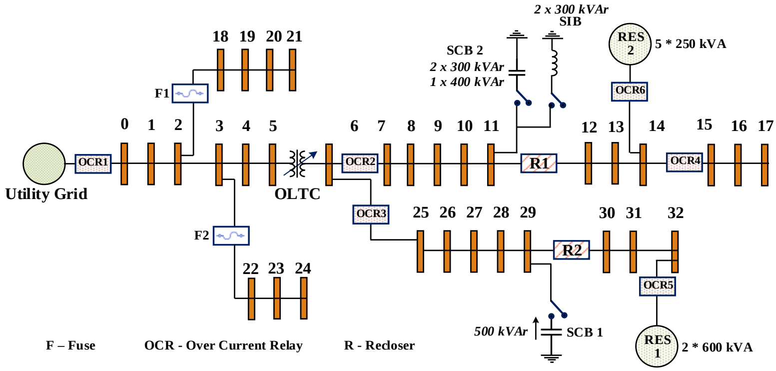

Fig. 8 – *Modified IEEE 33-bus distributed power system.*

In addition, OLTC and SCB units are connected to buses 5, and 11 respectively. The input voltage for the OLTC unit operation is considered bus 17, which is computed using the line drop compensation technique. The SCB and SIB units are activated based on their own bus voltage. Various fault situations, such as abrupt active power fluctuation (reduction in active power delivery at 15s), rapid load variation scenarios (addition of load at 20s, and load removal at 105s), are simulated using various voltage control techniques such as (a) voltage regulation of the DPS through OLTC only, (b) voltage regulation through the combined operation of OLTC and SCB/SIB units, (c) voltage regulation via the combined operation of OLTC, SCB/SIB, and DER units under IEEE recommended control. (d) Voltage regulation of the DPS through a proposed voltage control method. The test results are presented in Fig. 9. The voltage from buses 0, 7, 17, and 32 is measured for the purpose of analyzing the performance of each voltage control method. (i) During the OLTC grid voltage regulation method (shown in Fig. 9a), the OLTC unit is activated after 35s from the fault occurrence and during the period bus voltages are outside the safety margin (i.e., between 0.98 p.u. and 1.02 p.u.), specifically bus-32 has reached the low level of 0.905 p.u., which is very harmful to the electrical equipment connected to this bus system. In this method, OLTC tap changing units are operated three times (during the addition of load) to bring the grid voltage back to the specified safety range level. It is measured that the total time taken to reach the safety voltage region after the fault occurrence is about 50 s. (ii) At combined voltage regulation through OLTC and SCB (shown in Fig. 9b), the SCB unit is initially operated, and it takes 22s for the initial operation and a total of 35 s to return to the specified safety voltage margin. In this control, SCB had two switching operations, and OLTC achieved two tap changing operations to reach the safety voltage margin level. (iii) The combined voltage regulation through OLTC, SCB, and DER unit conventional reactive power control is shown in Fig. 9c.

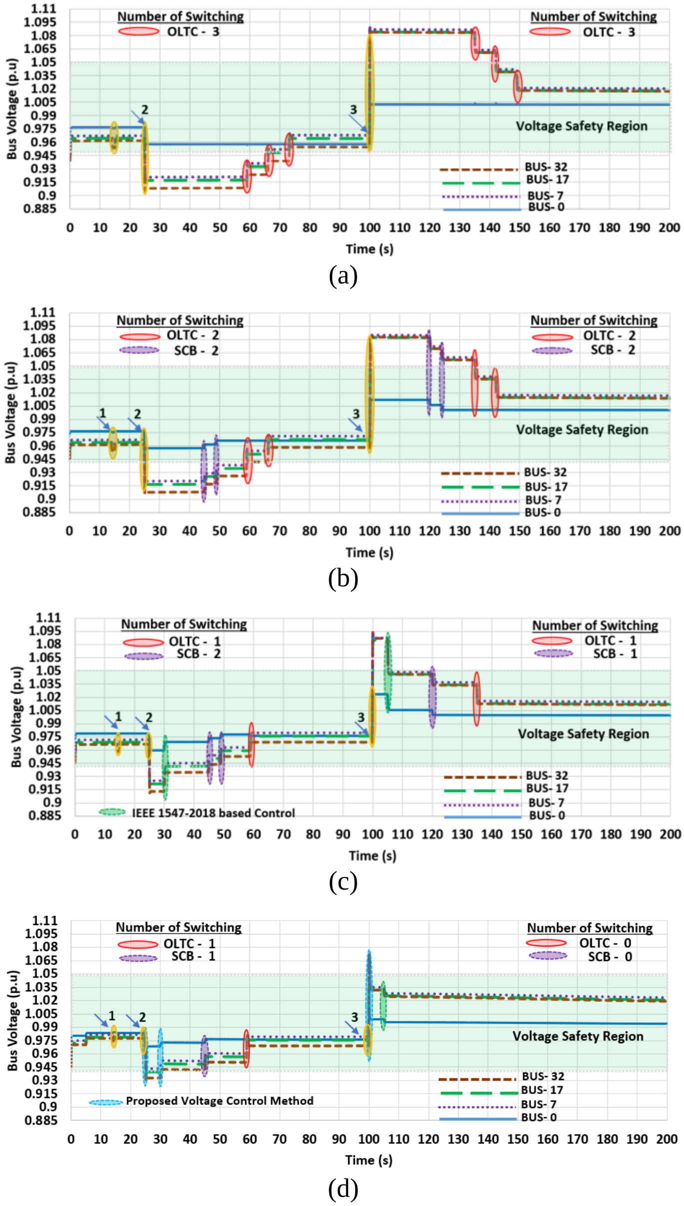

Fig. 9 – *Performance comparison of voltage control methods:* (a) *grid voltage control through OLTC;* (b) *grid voltage control through OLTC and SCB;* (c) *grid voltage control through the combined operation of OLTC, SCB, and DER unit reactive power control with IEEE recommended;* (d) *Proposed grid voltage control.*

The DER unit is initially operated at 5s and provides 0.44 p.u. of the reactive power support. Therefore, bus voltages are taken back from a very low level to a moderate level after the 5s (e.g., the voltage for bus 32 is moved to 0.932 p.u. from 0.915 p.u. voltage). In this voltage regulation method, OLTC and SCB units are operated at a single and two times, respectively. (iv) In the proposed voltage control method, DER units have instantly provided reactive power support to the DPS once the fault occurs. Therefore, bus voltages are not moving to the very low level (e.g., the low level for the voltage in bus-32 is 0.93 p.u., whereas it reaches as low as 0.915 p.u. for the remaining voltage control method). In addition, all the bus voltages are backed to 0.95 p.u. within 5s. Afterward, SCB and OLTC units are operated at a single time each to make sure to reach the safety voltage margin.

5.2 Test System 2: A Practical 85-bus Northern Tamilnadu, Indian distributed power system.

In this section, the proposed voltage control method is validated against a conventional IEEE recommended reactive power control in DER unit using a practical 11 kV, 85-bus system (shown in Fig. 10) located in northern Tamilnadu region, India.

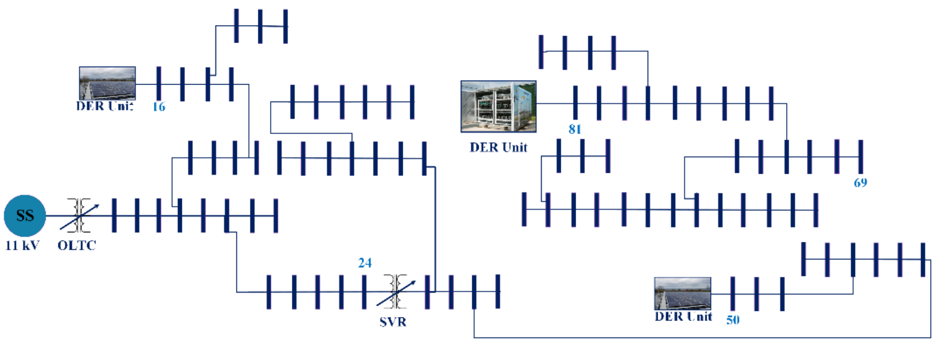

Fig. 10 – *Practical 85-bus distributed power system in Northern Tamilnadu, India.*

In this test system, OLTC units, step voltage regulators (SVR), and DER units are allowed to regulate the voltage in the DPS. The operational time delay for the OLTC unit is set as 60 s, and it has 16 taps with the accepted voltage safety region between 0.95 p.u. and 1.05 p.u., whereas the step voltage regulator is located on bus-24, and it has 33 taps with the accepted voltage region of 0.98 p.u. to 1.02 p.u. In this test system, three solar PV DER units are connected on buses-16, bus-50, and bus-81 with a rating of 1600 kVA, 1200 kVA, and 1800 kVA, respectively. The whole system is simulated for a day period (24 hours) in time domain simulation in MATLAB/Simulink. The comparison results for the conventional IEEE recommended reactive power control and the proposed reactive power control in the DER unit are presented in Fig. 11.

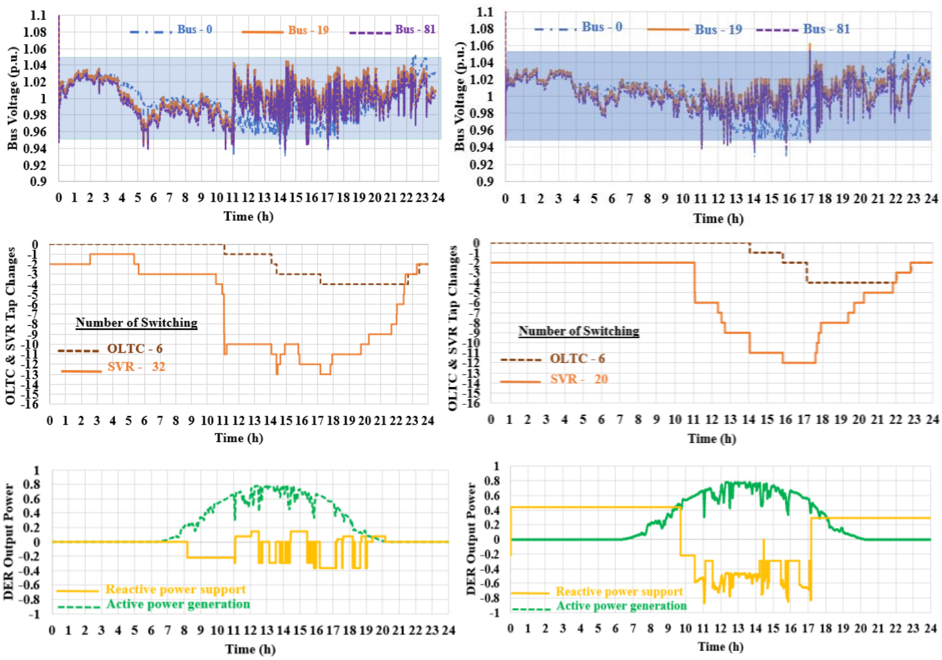

Fig. 11 – *Comparison of IEEE recommended reactive power control in DER unit* (a) *and proposed reactive power control in DER unit* (b) *for the DPS voltage regulation.*

In the conventional method, the DER unit is not able to provide reactive power support when active power generation is zero. Therefore, on-load tap changer and step voltage regulators are responsible for regulating the voltage in the DPS during the period and this leads to increasing the switching operations of the SVR unit. In 24 hours, proposed reactive power control in the DER unit has helped to reduce the switching operations of the SVR unit by 38% (i.e., the proposed reactive power control strategy achieved 20 switching operations while IEEE recommended reactive power control has provided 32 switching operations). In addition, bus voltage oscillations due to the load changes in the DPS are improved during the proposed voltage control method. For example, at 5.5 hours, the bus voltages are regulated at around 0.98 p.u. in the proposed voltage control, whereas in the conventional IEEE recommended voltage control, bus voltages are reached at about 0.955 p.u. When comparing reactive power support results in Fig. 11, the proposed reactive power control method immediately provided the reactive power support during active power generation.

6 Conclusion

The research demonstrated how to effectively use DER reactive power assistance for voltage control in a distributed power system through two test systems. The proposed reactive power control method in the DER unit reduces the switching operations of the SVR unit by 38% compared with the conventional reactive power control in the DER unit recommended by the IEEE work group. Furthermore, it has demonstrated the capacity of an embedded control system used for reactive power regulation of power converter-fed distributed energy resources. When compared with the various voltage control methods in the test systems, it is determined that the proposed voltage control improves grid voltage quality and lowers the number of switching operations of static voltage regulating devices, which leads to an increase in device life span. Furthermore, it reduces the amount of time spent beyond the voltage safety range.

7 References

[1] Renewable 2018, "Global status report -A comprehensive annual overview of the state of renewable energy, 2018, Available at: https://www.ren21.net/gsr-2018/.

[2] R. A. Walling, R. Saint, R. C. Dugan, J. Burke, Lj. A. Kojovic: Summary of Distributed Resources Impact on Power Delivery Systems, IEEE Transactions on Power Delivery, Vol. 23, No. 3, July 2008, pp. 1636 – 1644.

[3] A. Joseph, K. Smedley, S. Mehraeen: Secure High DER Penetration Power Distribution via Autonomously Coordinated Volt/VAR Control, IEEE Transactions on Power Delivery, Vol. 35, No. 5, October 2020, pp. 2272 – 2284.

[4] IEEE Std 1547™-2018, IEEE Standard for Interconnection and Interoperability of Distributed Energy Resources with Associated Electric Power Systems Interfaces, New York, USA, 2018.

[5] T. Stetz, F. Marten, M. Braun: Improved Low Voltage Grid-Integration of Photovoltaic Systems in Germany, IEEE Transactions on Sustainable Energy, Vol. 4, No. 2, April 2013, pp. 534 – 542.

[6] M. Kraiczy, T. Stetz, M. Braun: Parallel Operation of Transformers with on Load Tap Changer and Photovoltaic Systems with Reactive Power Control, IEEE Transactions on Smart Grid, Vol. 9, No. 6, November 2018, pp. 6419 – 6428.

[7] T.- T. Ku, C.- H. Lin, C.- S. Chen, C.- T. Hsu: Coordination of Transformer On-Load Tap Changer and PV Smart Inverters for Voltage Control of Distribution Feeders, IEEE Transactions on Industry Applications, Vol. 55, No. 1, January 2019, pp. 256 – 264.

[8] D. Ranamuka, A. P. Agalgaonkar, K. M. Muttaqi: Online Voltage Control in Distribution Systems with Multiple Voltage Regulating Devices, IEEE Transactions on Sustainable Energy, Vol. 5, No. 2, April 2014, pp. 617 – 628.

[9] T. Aziz, N. Ketjoy: Enhancing PV Penetration in LV Networks Using Reactive Power Control and On Load Tap Changer with Existing Transformers, IEEE Access, Vol. 6, February 2018, pp. 2683 – 2691.

[10] M. Kraiczy, M. Braun, G. Wirth, S. Schmidt, J. Brantl: Interferences Between Local Voltage Control Strategies of HV/MV-Transformer and Distributed Generators, Proceedings of the 28th European Photovoltaic Solar Energy Conference and Exhibition (EU PVSEC), Paris, France, September 2013, pp. 4217 – 4224.

[11] S. Satsangi, G. B. Kumbhar: Energy Savings Estimation of a Distribution System in Presence of Intelligent Volt-VAR Control based on IEEE Std. 1547-2018, CSEE Journal of Power and Energy Systems, Vol. 8, No. 5, September 2022, pp. 1477 – 1486.

[12] F. U. Nazir, B. C. Pal, R. A. Jabr: Affinely Adjustable Robust Volt/VAR Control without Centralized Computations, IEEE Transactions on Power Systems, Vol. 38, No. 1, January 2023, pp. 656 – 667.

[13] A. Savasci, A. Inaolaji, S. Paudyal: Two-Stage Volt-VAR Optimization of Distribution Grids with Smart Inverters and Legacy Devices, IEEE Transactions on Industry Applications, Vol. 58, No. 5, September 2022, pp. 5711 – 5723.

[14] G. C. Goodwin, S. F. Graebe, M. E. Salgado: Control System Design, Prentice Hall, Upper Saddle River, 2001.

[15] Y.- F. Liu, E. Meyer, X. Liu: Recent Developments in Digital Control Strategies for DC/DC Switching Power Converters, IEEE Transactions on Power Electronics, Vol. 24, No. 11, November 2009, pp. 2567 – 2577.

[16] H.- S. Youn, J.- S. Park, K.- B. Park, J.- I. Baek, G.- W. Moon: A Digital Predictive Peak Current Control for Power Factor Correction with Low-Input Current Distortion, IEEE Transactions on Power Electronics, Vol. 31, No. 1, January 2016, pp. 900 – 912.

[17] T.- F. Wu, T.- C. Chou, C.- W. Huang, K. Sun: Bi-Directional Grid-Connected Modular Multilevel Converters with Direct Digital Control and D-Σ Processes, IEEE Transactions on Power Electronics, Vol. 34, No. 11, November 2019, pp. 11290 – 11299.

[18] R. T. Ryan, D. N. Hogan, R. J. Morrison, J. G. Hayes: Digital Closed-Loop Control Strategy to Maintain the Phase Shift of a Multi-Channel BCM Boost Converter for PFC Applications, IEEE Transactions on Power Electronics, Vol. 34, No. 7, July 2019, pp. 7001 – 7012.

[19] S. Arora, P. T. Balsara, D. Bhatia: Digital Pulsewidth Modulation (DPWM) Using Direct Digital Synthesis, IEEE Journal of Emerging and Selected Topics in Power Electronics, Vol. 10, No. 4, August 2022, pp. 4231 – 4244.

[20] Y. Chen, W. Qiu, X. Liu, Y. Kang: A Parallel Control Framework of Analog Proportional Integral and Digital Model Predictive Controllers for Enhancing Power Converters Cybersecurity, IEEE Journal of Emerging and Selected Topics in Power Electronics, Vol. 10, No. 1, February 2022, pp. 1258 – 1269.

[21] S. Choudhury, B. Akin, M. Bhardwaj, Z. Yu: Digital Control of Dual Output Interleaved PFC Using Single Input Current Sense, Proceedings of the 28th Annual IEEE Applied Power Electronics Conference and Exposition (APEC), Long Beach, USA, March 2013, pp. 2225 – 2230.

[22] D. M. Brod, D. W. Novotny: Current Control of VSI-PWM Inverters, IEEE Transactions on Industry Applications, Vol. IA-21, No. 3, May 1985, pp. 562 – 570.